Analytical Methods

Accepted Manuscript

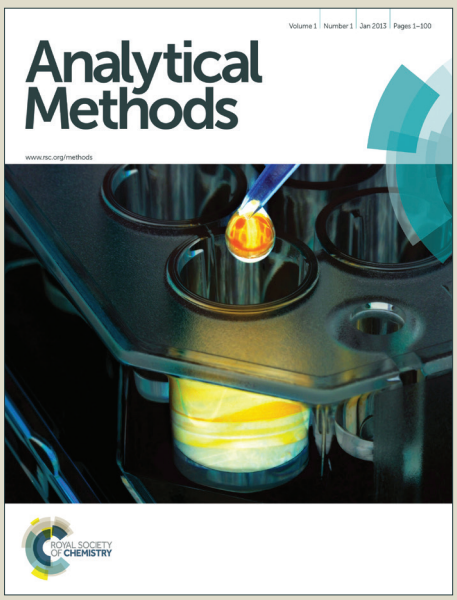

This is an *Accepted Manuscript*, which has been through the Royal Society of Chemistry peer review process and has been accepted for publication.

Accepted Manuscripts are published online shortly after acceptance, before technical editing, formatting and proof reading. Using this free service, authors can make their results available to the community, in citable form, before we publish the edited article. We will replace this *Accepted Manuscript* with the edited and formatted *Advance Article* as soon as it is available.

You can find more information about *Accepted Manuscripts* in the Information for Authors.

ROYAL SOCIETY OF CHEMISTRY

www.rsc.org/methods

Simple fluorescence-based detection of Cr (III) and Cr (VI) using unmodified Gold Nanoparticles

Elavarasi M, Sruthi Ann Alex, N. Chandrasekaran, and Amitava Mukherjee*

Centre for Nanobiotechnology, VIT University, Vellore, India

***Corresponding author**

Dr. Amitava Mukherjee

Senior Professor & Deputy Director

Centre for Nanobiotechnology

VIT University, Vellore - 632014

Email: amit.mookerjea@gmail.com

Phone: 91 416 2202620

Fax: 91-416-2243092

ABSTRACT

We present herein a fluorescence-based method for the determination of both trivalent and hexavalent forms of chromium in aqueous solutions using unmodified gold nanoparticles. The concept of the sensor was designed based on the aggregation of gold nanoparticles (Au NPs) by Cr (III), which resulted in a color change from red to blue and the appearance of a new secondary peak at 714 nm. The complexation of Au NPs by Cr (III) consequently led to the quenching of the fluorescence intensity of Au NPs proportional to the concentration of Cr (III). The Au NP aggregation upon the addition of Cr (III) has been correlated well with the mean hydrodynamic size measurements and scanning electron microscopic images. The system was found to possess a good linear correlation between the chromium concentration and the degree of reduction of fluorescence intensity (R^2=0.989) in the range of 10^{-7}–10^{-3} M and an excellent limit of detection of 10^{-7} M (5 ppb). The prospective application of our designed probe for environmental sensing can be highlighted as it has been found to successfully determine the chromium concentration in the real water samples. Our method has the advantage of cost-effectiveness and does not use any additional fluorophores for the sensitive detection of both forms of chromium.

KEYWORDS: Gold nanoparticles; Chromium (III); Fluorometric detection; Colorimetric sensor.

INTRODUCTION

Anthropogenic activities in the last few decades have brought about the release of effluents high in chromium and other heavy metals. The discharges from several industries like dye and pigment manufacturing, chrome plating, and leather and wood preservation are the major routes of entry into the environment.[1] The two most prevalent forms of chromium based on its oxidation state are Cr (III) and Cr (VI).[2] The trivalent form is an essential trace element which has a great influence on metabolizing lipids, glucose, and proteins and is required at low concentrations of 50-200 μg/dL/day.[3] However, at elevated concentrations, it can negatively impact the cellular components by crosslinking or binding to proteins and DNA to finally cause mutations that can lead to cancer.[4] The hexavalent form is more hazardous to humans due to its high solubility in combination with its carcinogenicity, and it can be easily taken up by the body. In compliance with the US EPA (Environmental Protection Agency), the hexavalent chromium concentration in drinking water should be below 0.1 μg/mL.[5] There are also possibilities for the transformation of Cr (III) into more lethal Cr (VI) under oxidizing conditions[6] that make the close monitoring inevitable for both forms of chromium in the environment.

Other analytical techniques like inductive-coupled plasma mass spectrometry (ICP-MS) and atomic absorption spectroscopy (AAS) suffer from drawbacks like high time consumption, expensiveness, and the requirement of sophisticated instrumentations[7] which can be circumvented by the use of our fluorometric approach for Cr (III) detection with the aid of unmodified Au NPs. Also, unlike the other methods which analyze the total chromium content of the sample, our technique can be used for the analysis of both Cr^{3+} and Cr^{6+}; however, the

accuracy and sensitivity of our technique fall short only in comparison to ICP-MS. In general, nanomaterial-based sensors are incorporated due to their simplicity, cost-effectiveness, and rapid determination of chromium in the environmental and biological samples. Gold nanoparticles are known for their exceptionally high plasmon resonance characteristics, excellent fluorescent properties, and strong extinction coefficient.[8] Several colorimetric methods have been used for the detection of both trivalent and hexavalent chromium.[9] Au NPs have been reported for the estimation of various metals like cadmium,[10] copper,[11] mercury,[12] lead[13] etc., which displayed a colorimetric response specific to the analyte.

The significance for the detection of Cr (III) and Cr (VI) in the environment has led to various developments in the field of nanosensors. In our previous study, we had used unmodified Au NPs on paper strips for the facile colorimetric detection of Cr (III) with an LOD of 1.53×10^{-7} M.[14] Hughes et al have constructed a 13-nm Au NP probe labeled with 5,5'-dithio-*bis*-(2-nitrobenzoic acid) for the detection of Cr (III) and achieved an excellent limit of detection of 5×10^{-10} M with the aid of Hyper Rayleigh Scattering.[15] Zhao et al have reported the use of Au NPs labelled using dithiocarbamate-modified N-benzyl-4-(pyridin-4-ylmethyl)aniline ligand for the determination of Cr (III) with a minimum detectable concentration of 6.2×10^{-7} M and can be further used for the indirect estimation of Cr (VI).[16] Ouyang et al fabricated a carbon electrode supporting self-assembled flower-like Au NPs for the detection of Cr (VI) with a limit of 2.9×10^{-9} M.[17] Upconversion nanoparticles have been utilized by Liu et al for Fluorescence resonance energy transfer (FRET) assay and a detection limit of 0.8 nM was yielded for Cr (III).[18] Gold nanoclusters stabilized by glutathione were used for estimation of both Cr (III) and Cr (VI) by Zhang et al with a limit of 2.5×10^{-6} M and 0.5×10^{-6} M, respectively.[19] From these diverse studies,

it can be concluded that plasmon resonance properties of Au NPs have been used widely for sensing chromium in both the forms.

The usage of fluorometry for chromium sensing has recently gained a lot of momentum.[20-27] Various fluorophores for the fluorometric determination of chromium have been listed along with their detection limit in Table 1. It can be seen that our method provides a detection limit of up to 10^{-7} M for Cr (III), which is lower than the other organic fluorophore-based sensing strategies, and also lower than the US EPA prescribed limit for Cr (VI) in drinking water. Also, there has been no fluorophore-based method for detecting both Cr (III) and Cr (VI) in water in prior studies. In comparison to our own reported paper, wherein Ag NPs were used as a fluorescent probe for Cr (III) estimation, Au NPs have several advantages over Ag NPs.[28] Au NPs have been found to have higher extinction coefficient.[29] They have higher stability due to their chemical inertness, and thus, ions do not leach out unlike Ag NPs, which may alter the working of the probe. Also, the leaching of Ag ions may also have a deleterious effect on the environment.[30]

To the best of our knowledge, there have been no reports so far for a strategy wherein fluorescence-based sensing of Au NPs have been used for the estimation of both Cr (III) and Cr (VI). As an added advantage, our method does not use any costly organic extrinsic fluorophores nor any complex capping agents. This is a straightforward technique for the sensitive and selective estimation of both trivalent and hexavalent chromium. Complexation of Cr (III) with the Au NPs triggers the instantaneous aggregation leading to the quenching of the fluorescence properties and a red-shift in the fluorescence emission peak. The variation in the intensity of the red-shifted peak proportional to the chromium concentration was used as the sensing principle.

EXPERIMENTAL

Reagents and solutions

Distilled water from Milli-Q was used throughout the studies. Hydrogen tetrachloroaurate dihydrate ($HAuCl_2$) was purchased from SRL Pvt. Ltd and SD Fine Chemicals Ltd (India). Heavy metal salts were purchased from Himedia Laboratories Pvt Ltd (India). The heavy metal solutions of 1 mM were used for the selectivity experiments by mixing the requisite amount of salt with the Mili-Q water [salts used were chromium nitrate, potassium di-chromate, cadmium sulphate, cobalt nitrate, mercury chloride, magnesium chloride, manganese sulphate, nickel chloride, lead nitrate, ferrous sulphate, zinc sulphate, aluminum sulphate, copper sulphate]. Chromium nitrate was used to prepare the stock solution of trivalent chromium (10^{-2} M) and was serially diluted to obtain the required concentrations. Dilute hydrochloric acid solution [0.1 N] was used for the pH adjustments.

Synthesis of gold nanoparticles (Au NPs)

All the glassware used were washed thoroughly with Mili-Q water, air-dried and then used for the experiments. The Au NPs were synthesized based on the Turkevich method.[31] 100 mL of aqueous solution of 1 mM $HAuCl_4$ was allowed to boil for 15 min under rapid stirring. Then, 5 mL of 38.8 mM trisodium citrate was added drop-wise and the mixture was kept rapidly stirred for 15 min, till the appearance of intense color change from yellow to wine red. The resulting solution was let to cool to room temperature (27°C) and then centrifuged at 6000 rpm for 15 minutes to collect the supernatant for further use.

Characterization

UV-Visible Spectroscopy

The synthesized colloidal Au NPs were subjected to preliminary characterization using UV-visible spectroscopic techniques. The spectra were recorded on the UV-Visible spectroscope (UV-Visible Systronic-2204, India) in the range of 200 to 700 nm. Millipore water was used as a blank. The spectra recorded were then replotted using Microsoft Excel.

Fluorescence Spectroscopy

The fluorescence spectra of as-synthesized Au NPs were recorded using Agilent from 200 nm to 700 nm. The Au NPs were also interacted with 10^{-3} M of Cr (III) and the fluorescence spectra were recorded.

Particle Size Analysis

The particle size distributions of the as-prepared Au NPs and Au NPs after interaction with the Cr (III) of 10^{-3} M concentration were measured using a particle size analyzer (90 Plus Particle Analyzer, Brookhaven instruments Corporation, NY, USA). The particle size was determined by calculating the mean hydrodynamic diameter from the auto correlation function of the light intensity scattered from the particles undergoing Brownian motion. Around 3 mL of the synthesized Au NP colloids were subjected for analysis.

Scanning Electron Microscopy

The morphological features of the colloidal Au NPs and Au NPs interacted with the 10^{-3} M Cr (III) were characterized using a scanning electron microscope (S4000 Hitachi, Tokyo, Japan) at a voltage of around 10 keV.

Fluorescence Determination of Cr (III)

For the detection of Cr (III) in fluorescence spectrometer, 700 µL of Au NP solution was added to 300 µL of different concentrations of Cr (III) (10^{-7}–10^{-3} M). This method was observed to be pH specific. The concentration of Cr (III) in the solution was calculated by correlating the fluorescence intensity at 582 nm.

Fluorescence Determination of Cr (III) and Cr (VI)

The Cr (VI) was pre-reduced to Cr (III) by using 1 mM sodium borohydride and then the fluorescence intensities of various concentrations of Cr (VI) interacted with Au NPs was noted.

Statistical analyses

Each set of experiments was carried out in triplicate and the mean values with the S.D. were reported. The error limits of the experiments were strictly kept within ± 5% limits. Repetitions of experiments were done to check for reproducibility. One-way ANOVA with Bonferroni's multiple comparison tests was carried out using Microsoft Excel to determine the statistical significance of selected experimentally obtained results.

RESULTS AND DISCUSSION

Characterization of the particles before and after interaction with Cr (III)

The synthesized colloidal Au NPs gave a strong plasmon resonance band at 526 nm as reported by earlier studies.[14] After interacting with Cr (III) solution of 10^{-3} M, the particles immediately aggregated due to the cross-linking of Au NPs by Cr (III). This led to an intense color change from wine red to blue and the appearance of a second peak towards the right of the primary peak at 714 nm when observed with UV-visible spectroscopy [Fig. 1].

For additional confirmation for the aggregation of nanoparticles, scanning electron microscopy was carried out to note the morphological changes of the nanoparticles. The SEM images of Au NPs showed predominantly spherical shape before interaction [Fig. 2a], while after interacting with 10^{-3} M of Cr (III), there were aggregates as the Au NPs complexed upon aggregation [Fig. 2b].

The hydrodynamic size analysis of the particles also correlated with microscopic and the spectroscopic analysis. The particle size distribution of the as-synthesized particles were analyzed using DLS and the particles were found to be stable in solution with a mean hydrodynamic diameter of 31.178 nm [Fig. 3a] and after interaction of the Au NP colloidal solution with 10^{-3} M of Cr (III), there were aggregates, the size of which had an increased mean diameter of 59.837 nm [Fig. 3b].

Optimization of the analytical procedure

The effects of pH and volume ratio of the Au NP dispersion to Cr (III) concentration were studied under different ranges (details provided in Table S1, supplementary information). The optimum volume ratio for sensing was found to be when 700 µL of Au NPs were interacted with

300 µL of Cr (III) solution. As the pH of the solution plays a major role, we have carried out pH optimization experiments with various pH values to determine that pH 3.0 for Cr (III) and an as-synthesized pH 4.0 for Au NPs were most favorable (see Table S2, supplementary information) and the same were used throughout the studies.

Fluorescence Quenching studies of Cr (III) with Au NPs:

The coordination of Au NPs with Cr (III) had resulted in the reduction of the fluorescent properties of Au NPs, thereby resulting in the quenching of fluorescence intensity exhibited by Au NPs. Similar modification of the fluorescence emission levels of Au NPs have been observed by Yan et al. for the detection of Hg^{2+}.[32] The quenching effects of Au NPs with different concentration of Cr (III) from 10^{-7} M to 10^{-3} M were represented in Fig. 4. On interaction of AuNPs with the various Cr (III) concentrations, the color of the samples were found to change from wine red to blue. [see Figure S1, supplementary information] It can be noted that higher concentrations of Cr (III) caused the fluorescence emission levels to decrease proportionately. Thus, the extent of fluorescence quenching corroborated with the Cr (III) concentration. The fluorescence intensity was significantly quenched by the addition of Cr (III) to Au NPs which was determined by the Stern-Volmer relation. The Stern-Volmer equation can be used to determine the number of binding sites (n) and binding constant (K) when a molecule/ion independently binds to a definite number of sites on a macromolecule.[33]

Further, to plot the Stern-Volmer relation, a linear calibration curve was plotted for intermolar concentrations of the range 10^{-7} M–10^{-6} M of Cr (III) versus the fluorescence intensity ratio F/Fo (Fig. 5) and the K_{SV} was calculated. A good linear correlation (R^2=0.989) was observed and a detection limit of 10^{-7} M was calculated for the probe. The quenching effect of fluorescence

emission on Au NPs by Cr (III) when further investigated showed that this process is highly concentration-dependent and could be determined by the Stern-Volmer relation.[34] The sensitivity of Cr (III) towards Au NPs for quenching the fluorescence can be arrived from the equation.

The number of binding sites (n) and binding constant (K) of Cr (III) with Au NPs were calculated by using the equation:

$\text{Log } F_0.F/ F = \log K + n \log [Q]$ [35]

Here, the F and F_0 represent the fluorescence intensities with the presence and absence of Au NPs. K and n represents the binding constant and number of binding sites available on the Au NPs respectively and Q is the concentration of Au NPs. By linear fitting of the plot of log ($F-F_0/F$) versus log [Q], the value of n number of binding sites were 1.5786 and K number of binding constant were obtained from the slope and y-axis intercept (Fig. 6) were found to be 8.358. The quenching constant K is an indication of the sensitivity of the Au NPs towards the Cr (III) ions that help to quench the fluorescence of Au NPs.[34]

Effect of potentially interfering ions

To evaluate the specificity of the probe, we have tested if the probe gave any interference with other transition heavy metal ions. Cr (III) of 10^{-7} M concentration was compared with other heavy metal ion solutions namely, Cd^{2+}, Co^{2+}, Cu^{2+}, Fe^{2+}, Pb^{2+}, Hg^{2+}, Mg^{2+}, Al^{3+}, Mn^{2+}, Ni^{2}, and Zn^{2+} of a higher concentration of 10^{-3} M. No color change or peak shift in the fluorescence spectra was observed and this served as an additional confirmatory test to prove that this method is only specific to Cr (III). The quenching effect was observed to be more in the case of Cr (III) in comparison to other heavy metals. From Fig. 7, it can be observed that only trivalent chromium interacts with the designed probe and that no other metal ions showed much

interference in the detection. Thus, it can be clearly noted that other metal ions have relatively little influence on the fluorescence of the system, indicating that the developed fluorescence sensor exhibits considerable specificity only to Cr (III).

Fluorometric detection of Cr (VI) using Au NPs

The pre-reduction of Cr (VI) was carried out by using 1 mL of 1 mM sodium borohydride. 1 mL of different concentrations of Cr (VI) (10^{-7} –10^{-3} M) were interacted with sodium borohydride for 5 min and after reduction of Cr (VI) to Cr (III), the pre-reduced chromium were interacted with Au NPs and there was an immediate color change from wine red to blue and an emission peak was found at 582 nm by fluorescence spectroscopy. Since the sodium borohydride is a strong reducing agent ensuring complete reduction of Cr (VI) to Cr (III), the amount of pre-reduced Cr (III) detected can be directly linked to the amount of Cr (VI) that was present initially, and hence, this method can be exploited for the estimation of both forms of chromium. A linear calibration was plotted against concentration of the pre-reduced Cr (III) 10^{-6} M versus F/F_0 and the R^2= 0.975 was found to be good linear correlation (Fig. 8). It can be noted that as the concentration of pre-reduced Cr (III) increases, the fluorescence intensity ratio F/Fo also decreases proportionately i.e. higher the Cr (III) concentration, higher is the fluorescence quenching of Au NPs. The limit of detection of pre-reduced Cr (III) was also calculated to be 10^{-7} M. All the experiments were carried in triplicates and One-way ANOVA with Bonferroni's multiple comparison test (p value < 0.0003) was performed to assess the sensitivity of the assay

Mechanism of fluorescence determination of Cr (III)

The colloidal Au NP suspension has a citrate stabilizer. In fluorescence spectrum, the emission peak was obtained at 582 nm on interaction between Cr (III) and Au NP.[14] The as-synthesized Au NPs in aqueous solution were stabilized against aggregation owing to the strong electrostatic repulsion between the negatively charged citrate ligands on the surface of the particles. The observed aggregation of Au NPs can be mainly due to the chelation of citrate ions on the Au NPs by the added Cr (III) ions.[36] Theoretically, two citrate ions can be chelated by one Cr (III) ion, through one hydroxyl and two carboxyl groups in each citrate ion. Thus, Cr (III) can act as a cross-linking agent for one pair of citrate-coated Au NPs, thereby inducing the aggregation of Au NPs. Since this chelation happens specifically by Cr (III), this method is selective to the detection of trivalent chromium.[37] As the aggregation of Au NPs take place, the interparticle distance of Au NPs also changes, and the fluorescence emission levels of Au NPs also varies. The absorption frequency of the SPR band of Au NPs depends on the interparticle distance as well as aggregate size.[38] With increasing concentrations of Cr (III), the Au NPs come in proximity to each other, whereby the fluorescence level of the Au NPs decreases, resulting in the quenching of the fluorescence. Thus, Cr (III) can act as a quencher that modifies the fluorescence signal emitted by Au NPs.[39] The schematic representation of the mechanism has been provided in Fig. 9.

Analytical applications

Furthermore, to evaluate the performance of the fluorometric probe in real environmental matrices, tap water and lake water samples were analyzed. The fluorescence intensities at 582 nm for tap water and lake water were noted to be 562 and 523, both of which were found to

possess Cr (III) within the range of concentrations of 500-50 ppb.[14] The chromium concentrations in the real samples (i.e. tap water and lake water) were also analyzed using a reference method, namely atomic absorption spectrometry (AAS, graphite furnace). The chromium concentrations in tap water and lake water as determined by AAS were noted to be 187 and 125 ppb respectively (see Table S3, supplementary information). Thus, this validates our newly developed fluorescence detection method as the Cr (III) concentration determined by our method correlated well with the values obtained from AAS and also because the different matrices used did not affect the concentration of the chromium determined.

CONCLUSION

In summary, we have established a rapid, facile, and time-efficient sensing strategy for the detection of Cr (III) using Au NPs as a simple fluorophore without any surface modification. The interaction of Au NPs with Cr (III) leads to a color change from wine red to blue which indicates the aggregation of the Au NPs with a corresponding peak shift towards the right. Further, the pre-reduction Cr (VI) to Cr (III) using sodium borohydride can be used for the estimation of total chromium which is the highlighting aspect of this method. Up-to-date no reports exist for the speciation of chromium using fluorimetry and both Cr (III) and Cr (VI) were found to have similar linearity and detection limit (10^{-7} M). Hence, our method was found to be advantageous over existing probes as it uses the intrinsic fluorescence of Au NPs, and it is cost-effective, sensitive, and can be used for the speciation of both forms of chromium.

Acknowledgement

The authors would like to acknowledge the Water Technology Initiative program, Department of Science Technology, Government of India and SAIF, IIT Madras for microscopic analysis.

REFERENCES

1. K. Tirez, G. Silversmit, N. Bleux, E. Adriaensens, E. Roekens, K. Servaes, C. Vanhoof, L. Vincze and P. Berghmans, *Atmos. Environ.*, 2011, **45**, 5332–5341.
2. D. Basu, K. Blackburn, B. Harris, M. Neal and F. Stoss, Environmental Protection Agency, Springfield, VA, 1983.
3. W.T. Cefalu, F.B. Hu, *Diabetes Care*, 2004, **27**, 2741–2751.
4. Z. Meibian, C. Zhijian, C. Qing, Z. Hua, L. Jianlin and H. Jiliang, *Mutat. Res.*, 2008, **654**, 45–51.
5. California Department of Public Health, 2012. Chromium-6 in Drinking Water: MCL Update.
6. P. Chadra and K. Kulshreshtha, *Bot. Rev.*, 2004, **70**, 313–327.
7. A. Ravindran, M. Elavarasi, T. C. Prathna, A. M. Raichur, N. Chandrasekaran and A. Mukherjee, *Sens. Actuators, B*, 2012, **166–167**, 365–371.
8. M. R. Bindhu and M. Umadevi, *Spectrochim. Acta A*, 2014, **128**, 37-45.
9. L. Zhao, Y. Jin, Y. Liu and H. Zhu, *Anal. Chim. Acta*, 2012, **731**, 75–81.
10. J. Yin, T. Wu, J. Song, Q. Zhang, S. Liu, R. Xu and H. Duan, *Chem. Mater.*, 2011, **23**, 4756-4764.

11. X. He, H. Liu, Y. Li, S. Wang, N. Wang, J. Xiao, X. Xu and D. Zhu, *Adv. Mater.*, 2005, **17**, 2811-2815.

12. N. Ding, H. Zhao, W. Peng, Y. He, Y. Zhou, L. Yuan and Y. Zhang, *Colloid Surface A*, 2012, **395**, 161-167.

13. N. Ding, Q. Cao, H. Zhao, Y. Yang, L. Zeng, Y. He, K. Xiang and G. Wang, *Sensors*, 2010, **10**, 11144-11155.

14. M. Elavarasi, A. Rajeshwari, N. Chandrasekaran and A. Mukherjee, *Anal. Methods*, 2013, **5**, 6211-6218.

15. S. I. Hughes, S. S. Dasary, A. K. Singh, Z. Glenn, H. Jamison, P. C. Ray and H. Yu, *Sensor Actuat. B: Chem*, 2013, **178**, 514-519.

16. L. Zhao, Y. Jin, Z. W. Yan, Y. Y. Liu and H. J. Zhu, *Anal. Chim. Acta*, 2012, **731**, 75–81.

17. R. Ouyang, S. A. Bragg, J. Q. Chambers, Z. L. Xue, *Anal Chim. Acta*, 2012, **722**, 1–7.

18. B. Liu, H. Tan and Y. Chen, *Anal. Chim. acta*, 2013, **761**, 178-185.

19. H. Zhang, Q. Liu, T. Wang, Z. Yun, G. Li, J. Liu and G. Jiang, *Anal. Chim. Acta*, 2013, **770**, 140-146.

20. Z. Zhou, M. Yu, H. Yang, K. Huang, F. Li, T. Yi and C. Huang, Chemical Communications, 2008, **29**, 3387-3389,.

21. Y. Lei , Y. Su, J. Huo, *Spectrochim. Acta A*, 2011, **83**, 149– 154.

22. A. J. Weerasinghe, C. Schmiesing, E. Sinn, *Tetrahedron Lett.*, 2009, **50**, 6407–6410.

23. P. Saluja , H. Sharma , N. Kaur , N. Singh , D. O. Jang, *Tetrahedron*, 2012, **68**, 2289-2293

24. D. Karak, A. Banerjee, A. Sahana, S. Guha, S. Lohar, S. S. Adhikari and D. Das, *J. Hazard. Mater.*, 2011, 188, 274-280.

25. L. Wang, G. Bian, L. Dong, T. Xia, S. Hong, H. Chen, *Spectrochim. Acta A*, 2006, **65**, 123–126.

26. L. Zhang, C. Xu, B. Li, *Microchim. Acta*, 2009, **166**, 61–68.

27. M. Elavarasi, M. L. Paul, A. Rajeshwari, N. Chandrasekaran, A. B. Mandal and A. Mukherjee, *Anal. Methods*, 2012, **4**, 3407-3412.

28. K. Saha, S. S. Agasti, C. Kim, X. Li and V. M. Rotello, Gold nanoparticles in chemical and biological sensing. *Chem. Rev.*, 2012, **112**, 2739-2779.

29. S. Eustis and M. A. El-Sayed, *Chem. Soc. Rev.*, 2006, 35, 209–217.

30. Y. H. Lin and W. L. Tseng, *Chem. Comm.*, 2009, **43**, 6619-6621.

31. G. Frens, *Nature*, 1973, **241**, 20-22.

32. L. Yan, Z. Chen, Z. Zhang, C. Qu, L. Chen and D. Shen, *Analyst*, 2013, **138,** 4280-4283.

33. B. Hemmateenejad, M. Shamsipur, F. Samari, T. Khayamian, M. Ebrahimi and Z. Rezaei, *J. pharmaceut. biomed.*, 2012, **67**, 201-208.

34. J. R. Lakowicz and B. R. Masters, **13**, 9901, 2008.

35. Haugland RP. Handbook of fluorescent probes and research chemicals, 9th ed. Molecular Probes Inc, Eugene, OR, 1996.

36. Y. Ye, H. Liu, L. Yang and J. Liu, *Nanoscale*, 2012, **4**, 6442-6448.

37. T. Wu, C. Liu, K.J. Tan, P.P. Hu and C.Z. Huang, *Anal. Bioanal. Chem.*, 2010, **397**, 1273–1279.

38. K. A. Kang, J. Wang, J. B. Jasinski and S. Achilefu, *J. Nanobiotechnol*, 2011, **9**, 16.

39. S. Y. Park, S. M. Lee, G. B. Kim and Y. P. Kim, *Gold Bull.*, 2012, **45**, 213-219.

Figures Captions

Figure 1.The UV-Visible spectra of the Au NPs and Au NPs after interacting with 10^{-3} M Cr (III).

Figure 2a. The Scanning electron microscopic [SEM] image of Au NP un-interacted.

Figure 2b. The Scanning electron microscopic [SEM] image of Au NPs after interacting with 10^{-3} M of Cr (III).

Figure 3a. A particle size distribution of synthesized Au NPs

Figure 3b. A particle size distribution of Au NPs interacted with 10^{-3} M Cr (III).

Figure 4. A Fluorescence spectra of Au NPs after interaction with different concentration of Cr (III) [10^{-3}–10^{-7} M]

Figure 5. A Stern-volmer plot of Au NP quenching with different Cr (III) concentrations.

Figure 6. A logarithmic plots of Au NPs after interaction with Cr (III) representing the binding constant (K) and no. of binding sites (n)

Figure 7. A Comparison of fluorescence ratios of Au NPs with 10^{-7} M of Cr (III) and 10^{-3} M of different heavy metals [Cd^{2+}, Co^{2+}, Cu^{2+}, Fe^{2+}, Pb^{2+}, Hg^{2+}, Mg^{2+}, Al^{3+}, Mn^{2+}, Ni^{2+}, and Zn^{2+}].

Figure 8. A Linear correlation of Cr (III) versus. F/F_0 after pre reduction of Cr (VI) to Cr (III).

Figure 9. Schematic representation of the mechanism indicating the fluorescence quenching of Au NPs on interaction with Cr (III)

Table 1: Brief account of various fluorescence-based sensing methods for Chromium detection

Sensor probe	**Capping agent**	**Analyte**	**Detection limit (M)**	**References**
Rhodamine	Naphthalimide	Cr (III)	2×10^{-4}	[20]
Rhodamine	Polyamidoamine dendrimer	Cr (III)	1×10^{-5}	[21]
Rhodamine	Thiophene-2-furanaldehyde	Cr (III)	13×10^{-6}	[22]
Benzimidazole	Imine linked	Cr (III)	7.9×10^{-5}	[23]
9-Acridone-4-carboxylic acid	-	Cr (III)	9×10^{-6}	[24]
Terbium composite nanoparticles	Unmodified	Cr (VI)	1×10^{-7}	[25]
CdTe quantum dot	Glutathione	Cr (VI)	1.6×10^{-7}	[26]
Ag NPs	Unmodified	Cr (III)	2×10^{-9}	[27]
AuNPs (current method)	Unmodified	Cr (III) & Cr (VI)	1×10^{-7}	

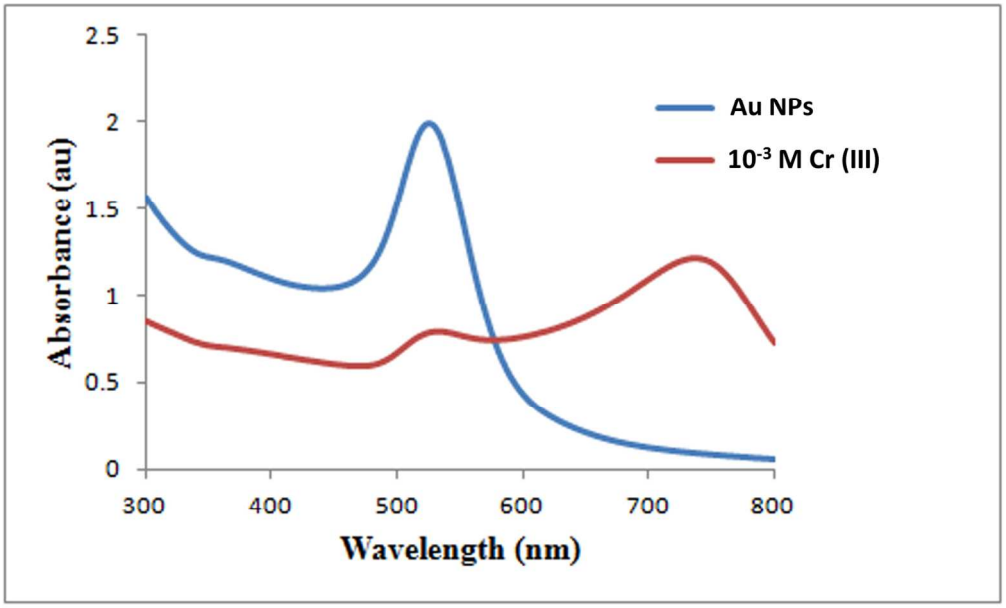

Fig 1
127x78mm (300 x 300 DPI)

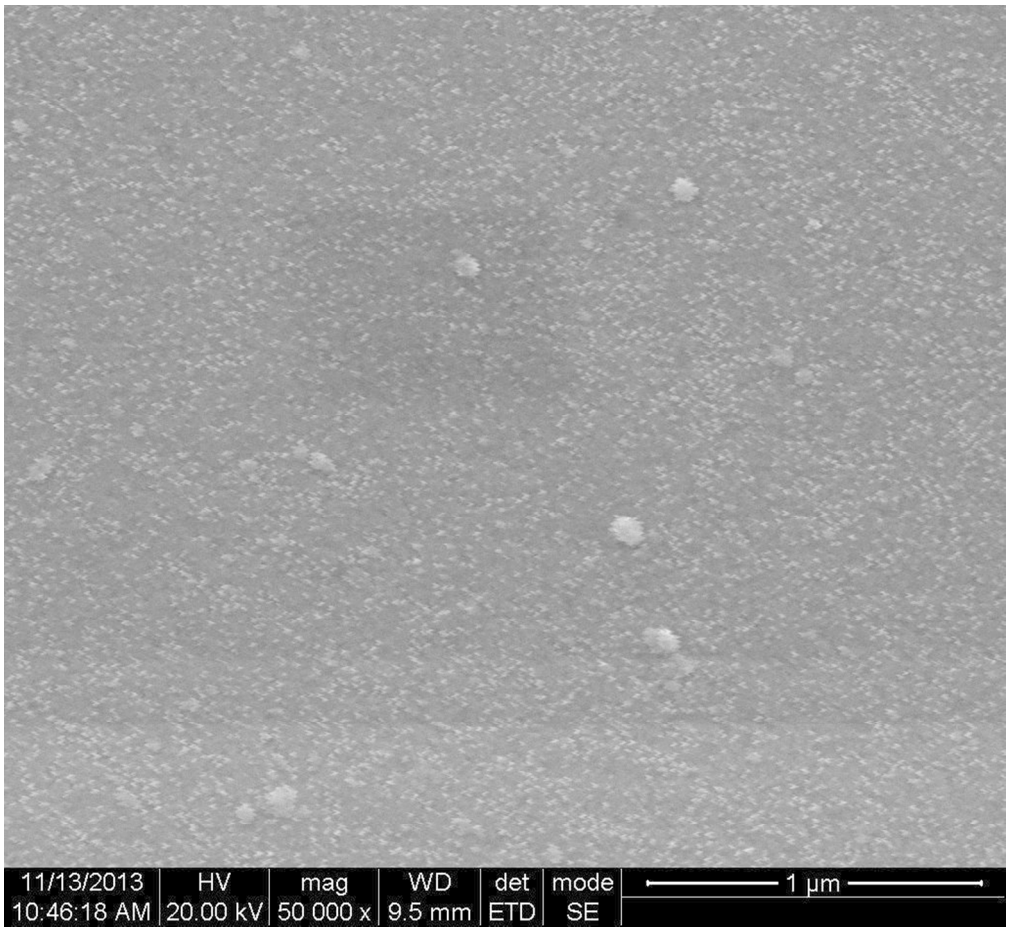

Fig 2a
361x332mm (72 x 72 DPI)

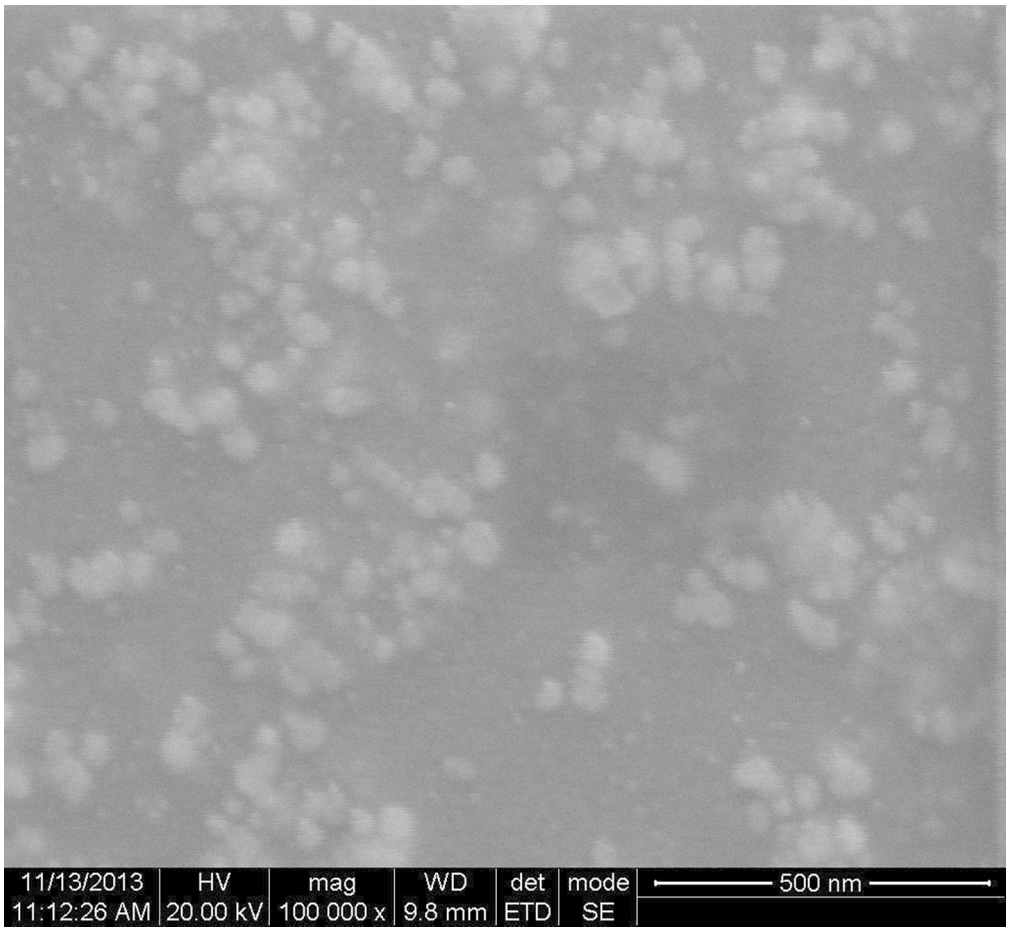

Fig.2b
361x332mm (72 x 72 DPI)

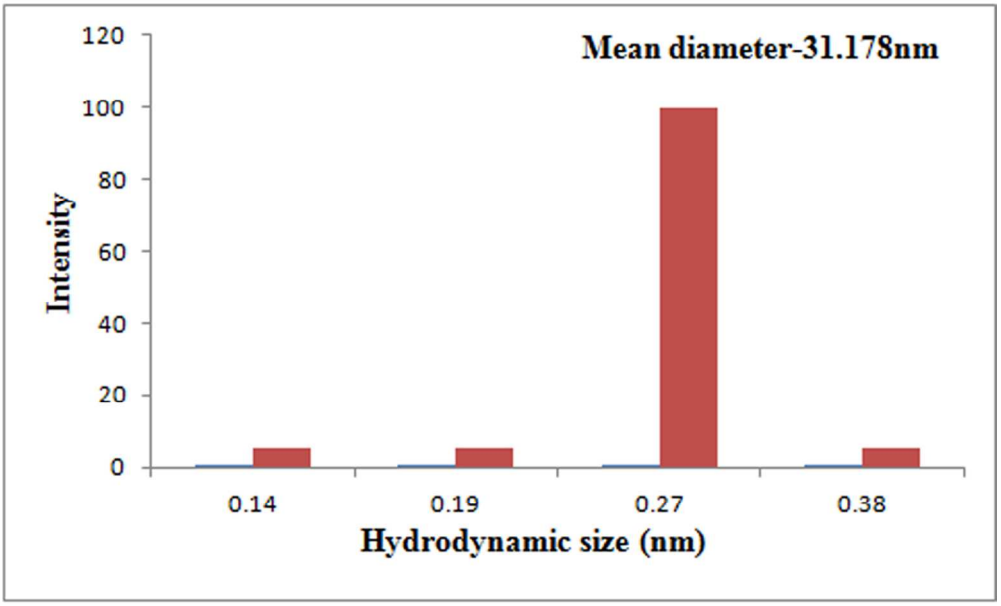

Fig. 3a
128x77mm (300 x 300 DPI)

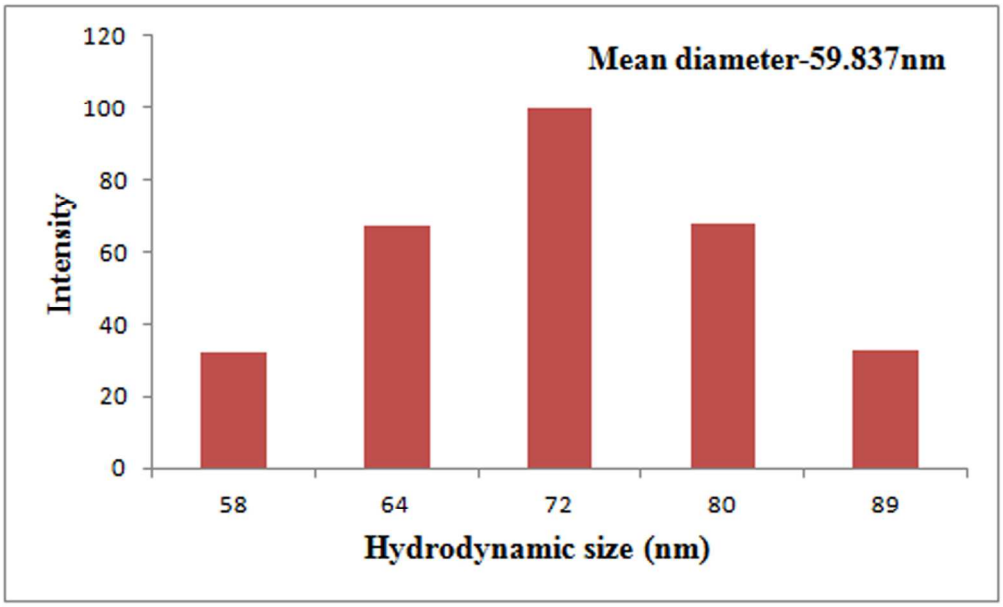

Fig.3b
128x77mm (300 x 300 DPI)

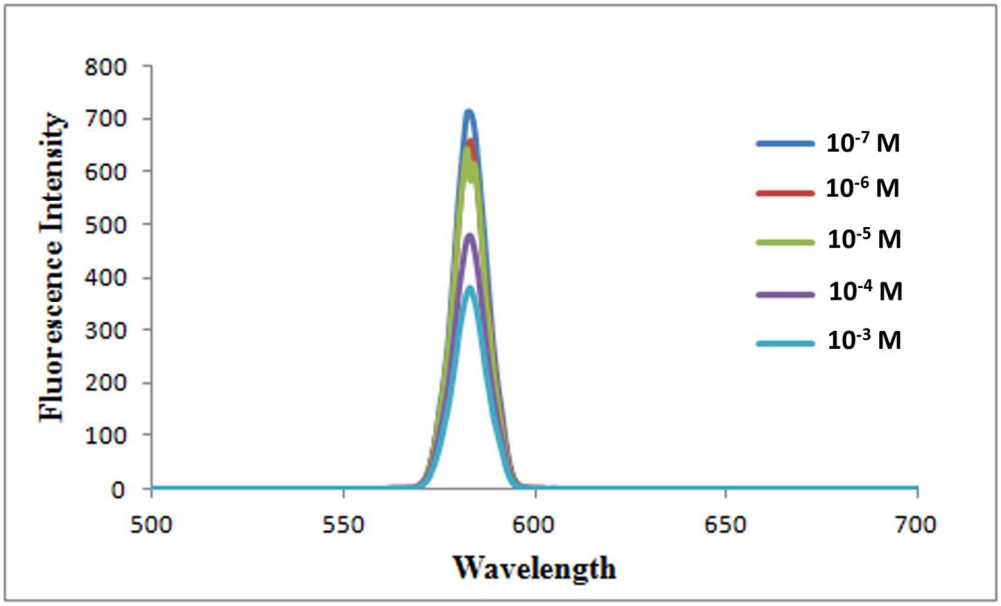

Fig.4
128x77mm (300 x 300 DPI)

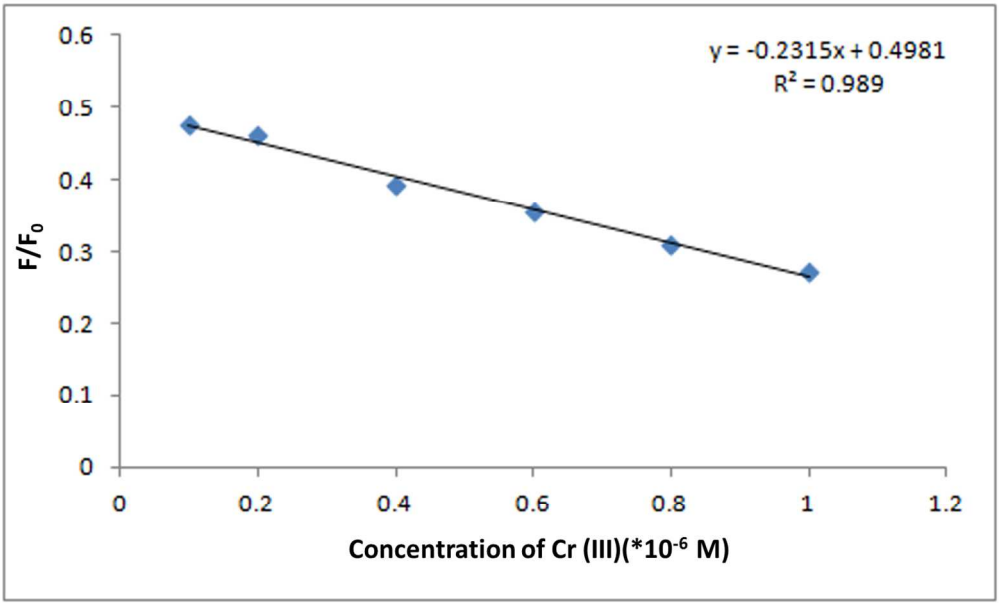

Fig.5
128x77mm (300 x 300 DPI)

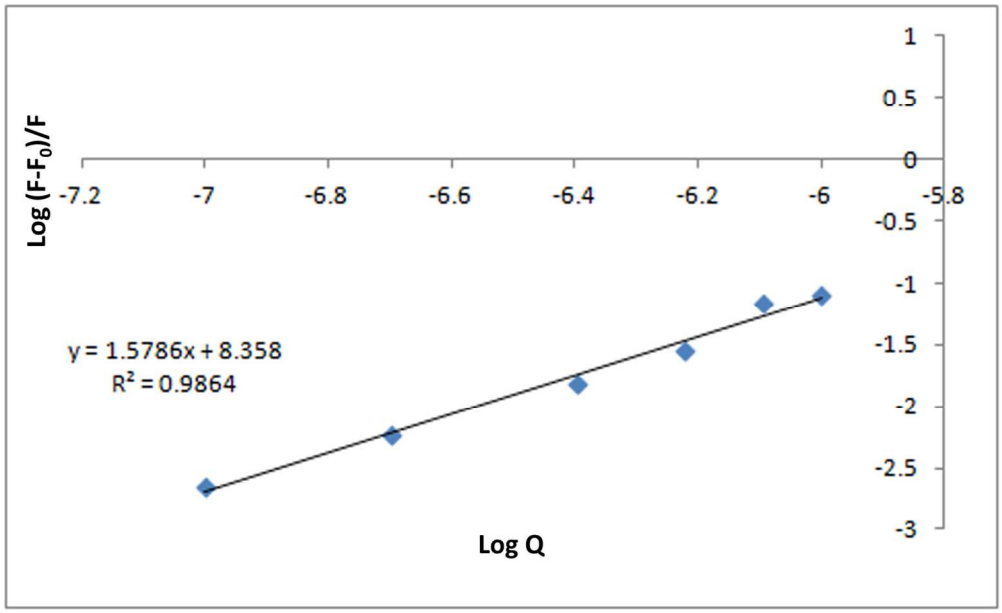

Fig.6
128x77mm (300 x 300 DPI)

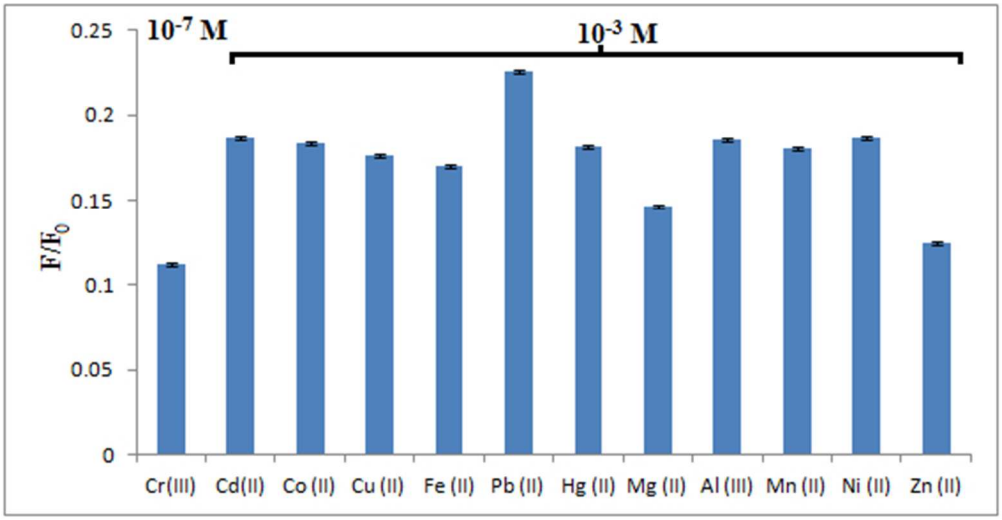

Fig.7
150x77mm (96 x 96 DPI)

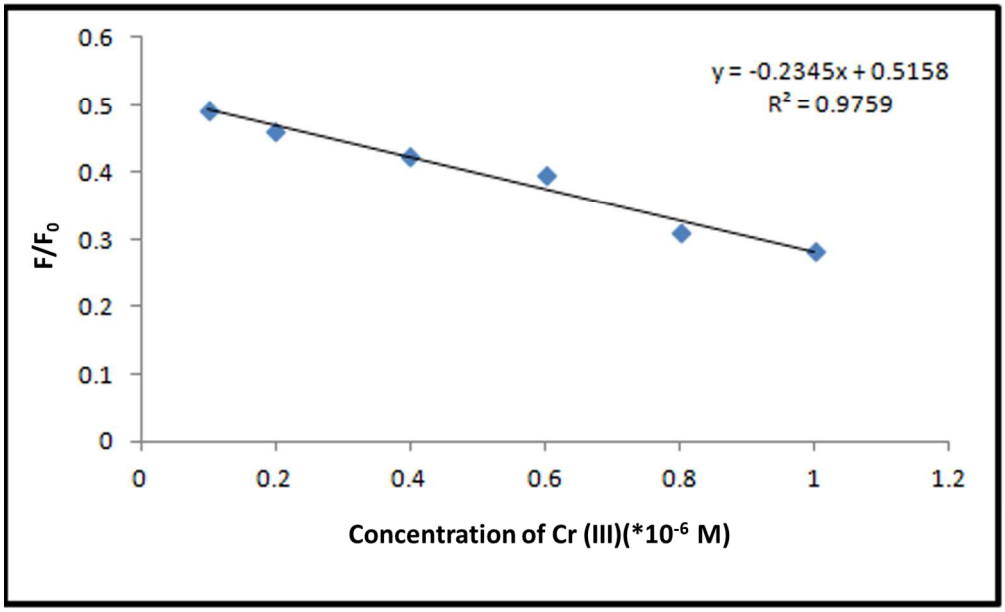

Fig. 8
127x78mm (300 x 300 DPI)

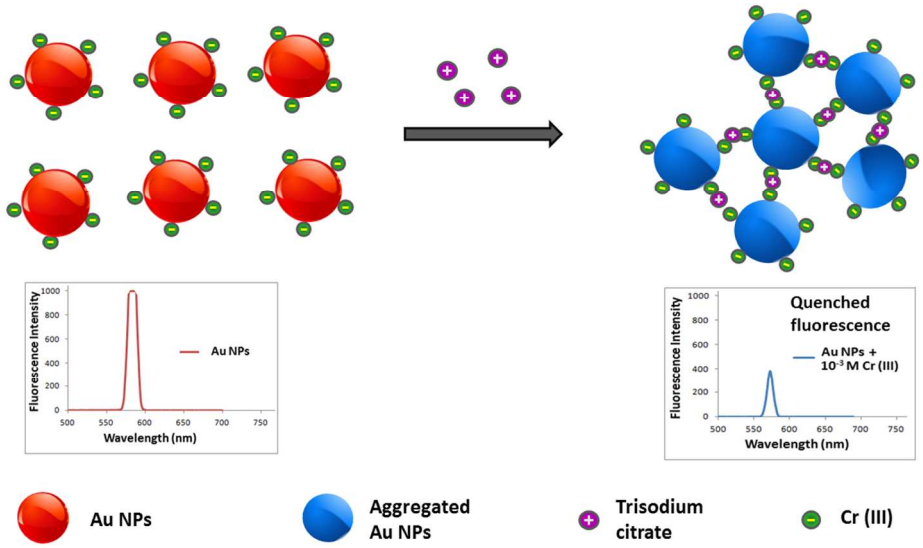

Fig 9
338x190mm (96 x 96 DPI)